International Journal of Nanoelectronics and Materials
IJNeaM
ISSN 1985-5761 | E-ISSN 2232-1535

Production of nickel oxide nanoparticles by laser and study of antibacterial properties against wound infection

Sara F. Abbas [a] *, Adawiya J. Haider [b], Sharafaldin Al-Musawi [c], Murtadha K. Selman [d], Jha Prafulla K [e], and Ali A. Al-Muntaser [f]

[a]*Laser and Optoelectronics Engineering Department, University of Technology- Iraq*
[b]*Applied Science Department/Laser Science and Technology Branch, University of Technology- Iraq*
[c]*College of Food Sciences, Al-Qasim Green University, Babylon Province, Iraq*
[d]*Ministry of Education - Babylon Education Directorate, Babylon Province, Iraq*
[e]*Department of Physics, Faculty of Science, M. S. University of Baroda, India*
[f]*Physics Department, Sana'a University, Yemen*
** Corresponding author. Tel.: +964-772-368-7684; e-mail: sarafadhel1989@gmail.com*

Received 09 July 2024, Revised 28 October 2024, Accepted 07 November 2024

ABSTRACT

Nanostructure materials have a variety of technical applications that come from their remarkable size-dependent properties as compared to particle range size. Nickel oxide (NiO) nanoparticles (NPs) acquire huge attention related to their promise usage in many fields. NiO NPs are produced using pulsed laser ablation (PLA) in distilled water (DW), a highly controlled and eco-friendly method. The manufactured NiO NPs were investigated by various techniques to study their physio-chemical properties. Structural analysis of NiO nanoparticles (NiO NPs) using X-ray diffraction (XRD) revealed that they possess a face-centered cubic (FCC) crystal structure. The formation of NiO NPs is indicated by Fourier transform infrared spectroscopy (FTIR) which presents a clear FTIR peak at 688 cm^{-1}. Field Emission Scanning Electron Microscope (FESEM) displays the common morphology with spheroids-like particles coalesced layer structure, and the mean particle size is 44 nm. Tauck's formula was employed to estimate the energy band gap, which was found to be aproximately 5.2 eV. Dynamic light scattering (DLS) shows that the particle size was 38.9 nm and that the NiO NPs had good stability. The zeta potential was negatively charged at 12.5 mV. Staphylococcus aureus (S. aureus) and Escherichia coli (E. coli) were examined for their antibacterial efficacy against the NiO NPs. The current investigation demonstrates strong antibacterial activity that may be investigated in the next clinical interventions.

Keywords: *Nanotechnology, Antibacterial, Nickel oxide, Laser ablation in liquid*

1. INTRODUCTION

Recently, nanotechnology has become the focus of scientists' attention due to its numerous technical applications in various fields [1–3]. Nanomaterials have incredibly interesting and practical qualities that come from their unique optical, electronic, and chemical properties [4], [5]. NPs have exhibited substantial antibacterial action, making them one of the most promising novel antimicrobial agents.

Alarming rates of antibiotic resistance are a result of the inappropriate and extensive use of antibiotics for both preventative and therapeutic purposes [6, 7]. Scientists are searching for novel antimicrobial medications as a result of developing antibiotic resistance of the common bacterial strains [8–10]. As a result, new antibacterial techniques must be developed to combat antibiotic-resistant microorganisms. Metals oxide nanoparticles (MeO NPs) are thought to be superior antibacterial medications because of their great stability, durability, and reduced toxicity to mammalian cells [11]. Various metals and metal oxides, like zinc, silver, copper, nickel, magnesium, titanium, etc., have ascended attention in environmental purification, food packaging, healthcare and biological and medical fields due to their ability to kill both bacterial strains [12, 13].

NiO is categorized as a p-type semiconductor with a wide energy gap ranging from 3.6 to 4.0 eV. NiO is used extensively in many different chemical and physical applications [14, 15]. These applications include gas sensors, adsorbents, electronics, catalytic materials, and magnetic and antibacterial agents [16].

Recent research concentrated on studying NiO NPs for their special qualities. NiO NPs exhibit encouraging promise in different biomedical applications. Research is being conducted to explore the antibacterial features of NiO NPs, along with their potential applications in cancer diagnosis and treatment. The antibacterial action of NiO NPs was studied by Ramasami *et al.* [17] against fungal (C. albicans) and (B. cereus and K. aerogenes) bacterial strains. Talebian *et al*. [18] investigated the antibacterial action of NiO NPs versus food-borne *S. aureus and E. coli* bacteria. Vijaya Kumar *et al*. evaluated the antibacterial efficacy of NiO NPs versus a wider variety of harmful microorganisms [17]. Isa Khan *et al.* [19] used NiO NPs to demonstrate how sensitive bacteria are to various bacterial strains (such as *S. aureus*

and E. coli). Using the agar diffusion method, Helan *et al.* [20] verified the cytotoxic effect of NiO NPs towards pathogenic bacteria including *S. aureus and E. coli*. NiO NPs differ greatly from bulk concerning their physio-chemical characteristics because of their quantum size and surface effects [21]. The compounds, including NiO NPs, have been applied extensively in several investigations, and their characteristics and uses have been thoroughly documented up to this point [22, 23]. Specifically, NiO NPs have generated an interest in biological and medical sciences due to their great biological properties, including their low cytotoxic impact. Because of their distinctive characteristics, they are more appropriate for applications where common materials have high toxicity or ineffectiveness. Nevertheless, there is a dearth of thorough research on the antibacterial qualities of NiO and its nanostructure. Understanding the safety and effectiveness of NiO NPs more in detail can make them important tools for the future development of nanomedicine [23].

The mechanism of antibacterial activity of MeO NPs is not recognized [24]. The antibacterial features of NiO NPs are mediated by several methods. Reactive oxygen species (ROS) production upon contact with bacterial cells is one of the most important mechanisms. These ROS cause oxidative stress, which harms lipids, proteins, and DNA in cells and eventually kills the bacteria [25, 26]. The heightened antibacterial activity of NiO NPs is partly owed to their unique nanostructure characteristics, which contain high surface area-per-volume proportion and small size. All these collective actions render NiO NPs highly potent against bacteria inclusive of antibiotic-resistant strains and biofilm-associated bacteria. It also minimizes the chances that encountered bacteria will develop resistance to a particular target; thus, NiO NPs may find useful applications in the fields of medicine and other applications such as in the development of medical equipment and materials, wound healing dressings, and coatings. These characteristics let the nanoparticles engage with bacterial cells more effectively, which raises their effectiveness [27].

Many methods are used to produce NiO NPs, such as sol-gel, microwave irradiation, solid-state reaction, thermal decomposition, laser ablation, etc. [28–30]. Of all the mentioned synthesis processes, the PLA method has many advantages. In PLA, strategies for regulating pressure or heat are not necessary [31–33]. PLAL is a versatile method for producing many types of NPs, including semiconductors, alloys, oxides, and noble metals [34–36].

This technique involves developing a plasma plume that is fully immersed in a liquid medium while utilizing high-intensity PLA to establish an interaction between laser matter and the target's surface [37, 38]. The PLA method and plasma produced are shown in Figure 1(c).

This study aimed to utilize a straightforward method to produce NiO NPs as an effective antibacterial agent and examine their impact on common wound-associated pathogenic bacteria. The research showcases the fabrication of NiO NPs using the PLA method, presenting results from structural, optical, chemical, and zeta potential characterization analyses. Additionally, it offers insights into the antibacterial effectiveness of NiO NPs against the pathogenic strains associated with wound infections. This comprehensive investigation details the various properties of NiO NPs and emphasizes their potential for diverse biological applications, particularly in wound care and antibacterial treatments.

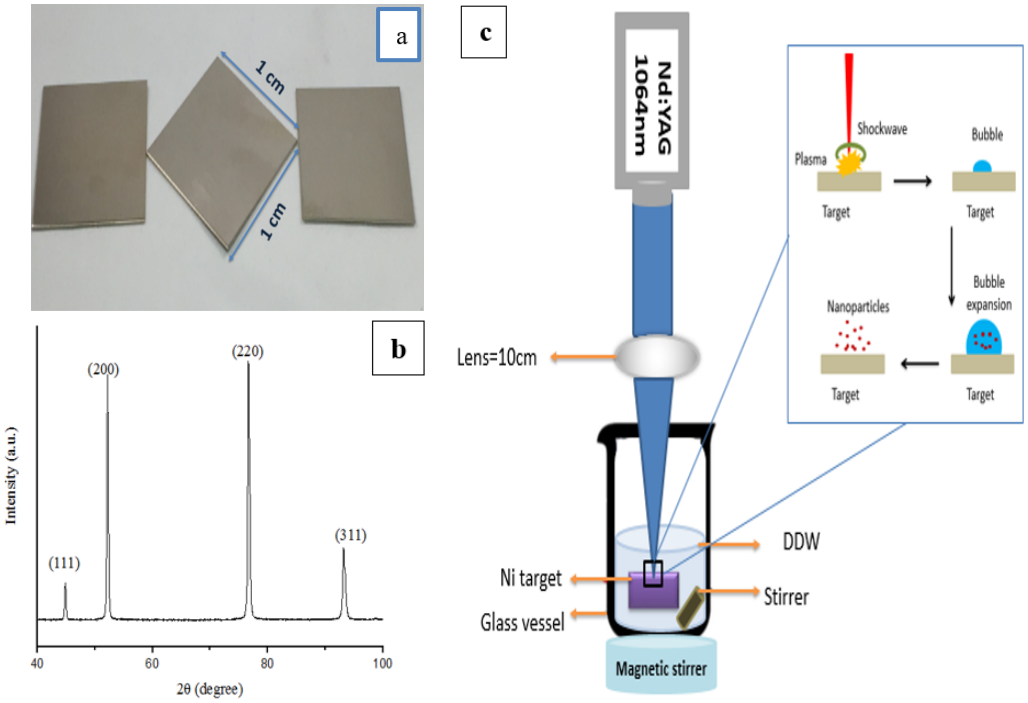

Figure 1. (a) Nickel sheet after cutting. (b) XRD analysis of the nickel sheet. (c) Schematic of PLA process

2. SAMPLE PREPARATION METHOD

A high purity (99.999%) nickel sheet was supplied from (BDH Chemical Ltd pool, England). The XRD pattern of the nickel target is shown in Figure 1(b). The PLA method was employed in this work to produce nanostructured NiO. The metal sheet was cut into small parts (1x1) cm, as seen in Figure 1(a). The nickel target was cleaned by using methanol and DW. The target was put inside a glass container that had (5 ml) of DW. In this method, a Q-switched Nd:YAG laser (Huafei Tongda Technology, DIAMOND-288 model EPLS) with a wavelength of 1064 nm, pulse duration of 10 nanoseconds, and repetition rate of 1 Hz was used to generate the nanostructure. A convex lens with a 10 cm focal length was employed to focus 32 J/cm^2 laser fluence for every pulse onto the target while mechanical stirring was applied during the process. Five experiments were repeated for each sample, so the results were similar.

3. CHARACTERIZATION TECHNIQUES

Different methods were applied to study the properties of the produced NiO NPs. The XRD pattern of the NiO NPs was analyzed using an AERIS PAN alytical XRD instrument with a Cu-Kα radiation source, over a 2θ range of (10–80) degrees. FTIR spectroscopy using the 8000 Series Shimadzu was employed to detect bond vibrations of the NPs in the 400–4000 cm^{-1} range. A double-beam UV VIS spectrophotometer (Shimadzu UV-1800) was used to record the the optical absorption spectrum, and the energy band gap was determined using Tuac's formula. The nanostructures' morphology was examined using an Axia ChemiSEM SEM. EDX was used to verify the chemical construction of the prepared sample. DLS (Malvern Zetasizer ZS, Malvern, UK) was used to determine the particle diameter and zeta potential.

4. ANTIBACTERIAL ASSAY

The agar well diffusion assay was employed to study the antibacterial qualities of the NiO NPs and determine their characteristics. It was based on Selecting these bacteria, namely *S. aureus and E. coli*, which belong to gram-positive and gram-negative groups, respectively. The amount of NiO NP solution (25, 50, 100, 150, and 200 µg/ml) was diluted in the experimental plates. After 24h of enculture in sterile Petri dishes at 37° C for each growth plate, the zone of inhibition was checked. By 24 h, the efficacy of the concentration was calculated, and the diameter of the growth inhibition was measured as encircling zones. Finally, the distance between the zone (mm) around each well was measured.

5. RESULTS AND DISCUSSIONS

The surface of Ni interacts with PLA to produce a plasma plume that splashes into liquid media. The alteration of water colour can provide an initial indication of the formation of NiO NPs. An intense shift in the absorption spectra of NiO NPs is observed around 250–300 nm, as shown in Figure 2. Determining the energy band gap is essential, as it provides insight into a material's electronic, optical, and thermal properties. The optical band gap of NiO is broader than that of the bulk (3.65 eV). This may relate to the quantum confinement phenomena; the peak absorption wavelength can change based on the size of the NPs. The absorption spectra change when the size of the NPs reduces because the electrons' energy levels become quantized. When it comes to absorption peaks, smaller NPs typically exhibit a bluer shift than larger ones. This effect results from the creation of new energy levels that increase the value of band gap energy because of gaps in the intergranular areas or chemical flaws [39]. The optical band gap was estimated using the standard Tauc's relation [40]:

$$(\alpha h\upsilon) = A\,(h\upsilon - Eg)^n \quad (1)$$

where "A" is a constant, and "hυ" is the incident photon energy, n equals ½ for direct transition. The intercept point at = 0 can be used to calculate the Eg value from the Plotting hυ on the x-axis and $(\alpha h\upsilon)^2$ on the y-axis, presented in Figure 2 (inset). The Eg value of 5.2 eV that NiO NPs had is consistent with the findings of other writers [17, 41].

FTIR was performed on the materials to determine their chemical bonds and functional groups. Figure 3 illustrates the FTIR spectra of NiO NPs as a synthesis that shows some significant absorption peaks. The peaks observed in Figure 3 are at 3435, 2071, 1634, and 688 cm^{-1}. The peak at 3435 cm^{-1} corresponds to the stretching vibrations of H_2O molecules, while the peak at 1634 cm^{-1} is associated with their bending mode [42, 43]. The investigation showed that the presence of carbon dioxide may have come from atmospheric contamination at 2071 cm^{-1}.

The peak at 688 cm^{-1} ascribes to NiO NPs Ni–O stretching vibration mode [44, 45]. Table 1 shows the FTIR information. Since the absorption band is so wide, the NiO NPs may be quite small and crystalline [46]. Because the particles studied in this work were much smaller than bulk NiO, the NiO NPs' IR peak of the Ni–O stretching vibration was moved near the blue region. This concept is relayed to the reduced size of particles, quantum confinement effects, or modifications to the surface [47].

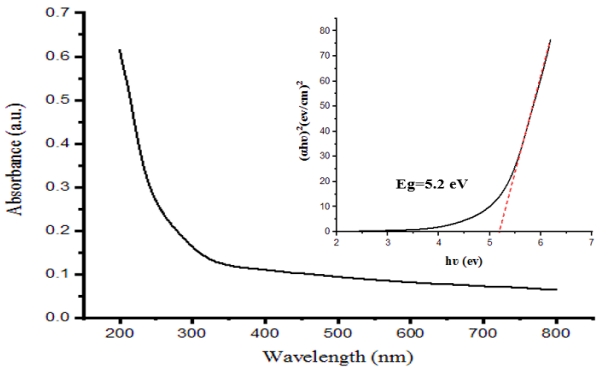

Figure 2. Absorption spectra of NiO NPs (inset: Eg of NiO by using Tauc's plot)

Table 1. Bond positions and functional groups of synthesized NiO NPs

Wavenumber (cm^{-1})	Bond type
3435	O=C=O Stretching
2071	O=C=O Stretching
1634	O–H Bending-Vibrational
688	Ni–O stretching-vibrational

Table 2. The structural properties of NiO NPs

2θ	(hkl)	Crystal size (Å)	D-spacing (Å)
38.4°	(111)	184	2.33971
44.9°	(200)	526	2.01509
77.8°	(311)	222	1.23952

XRD analysis of the samples' crystal structure, phase composition, and particle size makes it possible to predict and modify the antibacterial performance of the material. XRD procedure was applied to determine and verify the crystallinity structure of the produced NiO NPs. The XRD pattern of the synthesized NiO nanoparticles by the PLA method is presented in Figure 4. The XRD patterns showed no further impurity peaks. The given reflections represent a crystalline structure face-centred cubic (FCC). The XRD pattern of NiO NPs shows characteristic peaks at 2θ = 38.4°, 44.9°, and 77.8°, corresponding to hkl values (111), (200), and (311) respectively. These diffracting peaks match the standard card number NiO (JCPDS 47-1049), which indicates nickel oxide has been created. The diffraction peaks have widened, indicating a tiny crystal size. The location and strength of these peaks, as determined by XRD analysis, reveal important details regarding the crystalline structure of the produced NiO NPs. The diffraction peak 2θ = 52.2° corresponds to the (102) plane representing the formation of Ni (OH)2 (JCPDS 14-0117). For the determination of particle sizes, the Debye-Scherrer formula has been employed [48]:

$$D = (0.9\lambda)/\beta\cos\theta \quad (2)$$

In this context, D represents the crystallite size, θ is Bragg's angle, λ is the wavelength of the radiation used, and β is the full width at half maximum (FWHM) of the diffraction peak. Table 2 shows the full information of NiO NP diffraction peaks.

The results of the previous analysis indicate that there is a relation between the topographical surface properties of NiO NPs and their appropriateness for biological efficiency. These special characteristics of the synthesized NiO NPs can be managed and described, allowing for the biocompatible particles to be designed for specific medical and therapeutic purposes based on how they will engage with living systems. The surface morphology of NiO NPs prepared by drying the suspended nanoparticles onto a glass substrate have been investigated using FESEM, as represented in Figure 5(a). According to several earlier investigations, MeO NP nanoparticles with sizes in the range of 1 to 100 nm and a variety of morphologies are effective antibacterial agents against infectious illnesses [49]. The NiO nanoparticles produced in this study exhibited a semispherical shape and showed agglomeration, with an average size of 44 nm, as observed in the FESEM micrograph. Thus, the nanoparticles produced in this work may represent a promising class of antibacterial agents. Image analysis, especially by software like ImageJ to measure the size distribution of NPs is well well-accepted and reliable technique in material science which is presented in Figure 5(b).

EDX is used to ascertain the fundamental basic synthesis elements of NiO NPs. Figure 6 displays the EDX spectrum for the NiO NP sample. The peaks in the spectrum of EDX between 0 and 2 keV showed that NiO NPs were synthesized effectively, according to existing findings [24, 50] since the only elements found are O, C, and Ni. The elemental analysis is displayed in the inset table of Figure 6, where the atomic percentage ratios for C, O, and Ni were 13.4, 47.5, and 39.1, respectively. These observational data collectively show that NiO NPs are prepared effectively. The elemental maps for EDX are displayed in the inset images of Figure 6. Each map is expressed in terms of colour representation of each constituent of the map as rendered in its brilliance (elementary) and black (element scarcities) maps. The elements show a uniform and consistent distribution over the whole measured region.

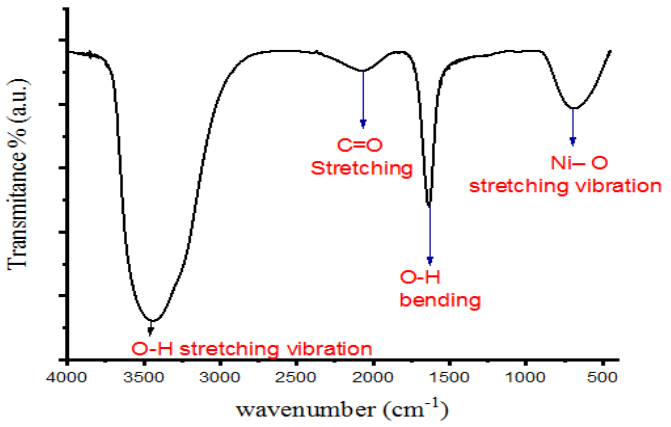

Figure 3. FTIR spectra of NiO NP suspension

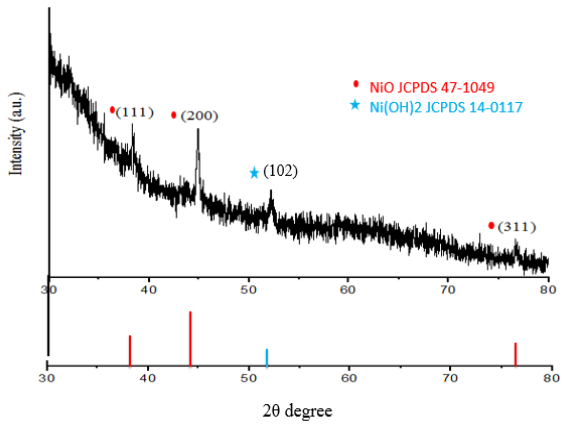

Figure 4. XRD analysis of NiO NPs with reference cards pattern

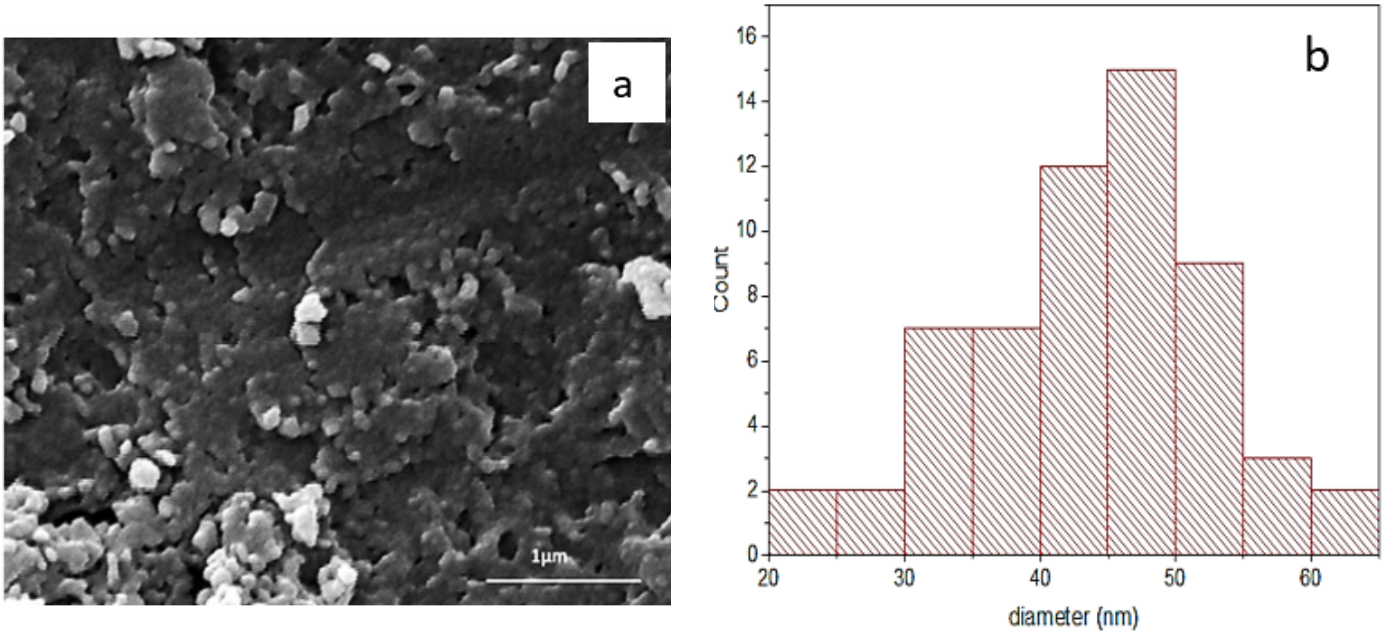

Figure 5. (a) SEM images of NiO NPs. (b) Particle size distribution

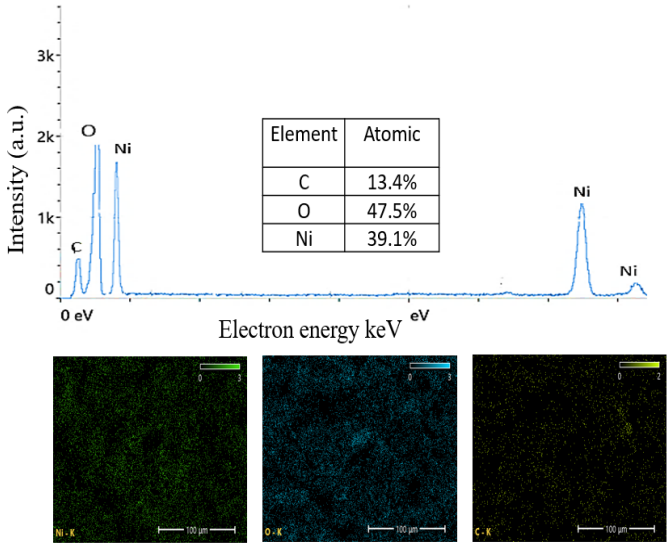

Figure 6. EDX image of NiO NPs

The zeta potential measurement of NiO NPs manufactured by PLA is shown in Figure 7.a. The zeta potential was used to estimate synthesized NiO NPs' stability in the colloidal solution. It shows how strongly particles with the same charges repel one another in the dispersion medium. Higher negative charges were found to be related to an increase in stability; that is, the greater the negative charge of NPs, the more stable they were [51]. In the current study, the negative sign of zeta potential was found (–12.5) mV. This reveals that NiO NPs produced by PLA are moderately stable. Bacterial cell walls and membranes are mostly negatively charged. The MeO NPs with positive charge and bacterial surfaces are attracted to each other due to attraction via the electrostatic interaction. Even particles with a negative zeta potential are capable of disturbing cell membranes. Therefore, interaction forces may be hydrophobic, Van der Waal, and electrostatic [52].

Figure 7(b) represents the size distribution of the NiO NPs suspension. The average particle size found for NiO NPs was 38.92 nm. It was shown that the mean size of NiO NPs obtained according to the analysis. The size ascertained by FESEM was larger than the one ascertained by DLS. The differences in the FESEM and DLS analysis conditions could account for the result situations. DLS measurements were accomplished in an aqueous medium, while FESEM analysis was done on dried samples. The drying process may influence the particle diameter determination.

The poly-dispersity index (PDI) can be assumed to be an important indicator that shows the homogeneity of the NP sizes in the sample. The PDI scale ranges from 0 to 1 [53]. A PDI value of less than (0.4) indicates that the suspension is homogeneous [54]. However, a suspension is considered exceedingly varied if the PDI value is greater than one [55]. The PDI recorded in this work was 0.189, showing that the particle size distribution of the generated NiO NPs was narrow and homogeneous. This shows that a major fraction of the NiO NPs had comparable diameters, resulting in a well-defined size distribution.

Numerous reports have been published by the research community on the application of NiO NPs in various biomedical fields. The NPs were employed as both antibacterial and antifungal agents. Thus, the cytotoxic effect and favourable biological properties of NiO NPs make these applications possible. In the present study, *S. aureus* and *E. coli* bacteria were used to examine the antibacterial behaviour of NiO NPs synthesized. The agar well diffusion assay was used to observe the growth of bacteria in culture media containing varying doses of NiO NPs by evaluating the diameter of the inhibition zone using vernier. The antibacterial properties were examined at different NiO NP concentrations (25, 50, 100, 150, and 200) µg/ml. At lower concentrations, when compared *to E. coli, S. aureus* demonstrated a greater sensitivity to NiO nanoparticles.

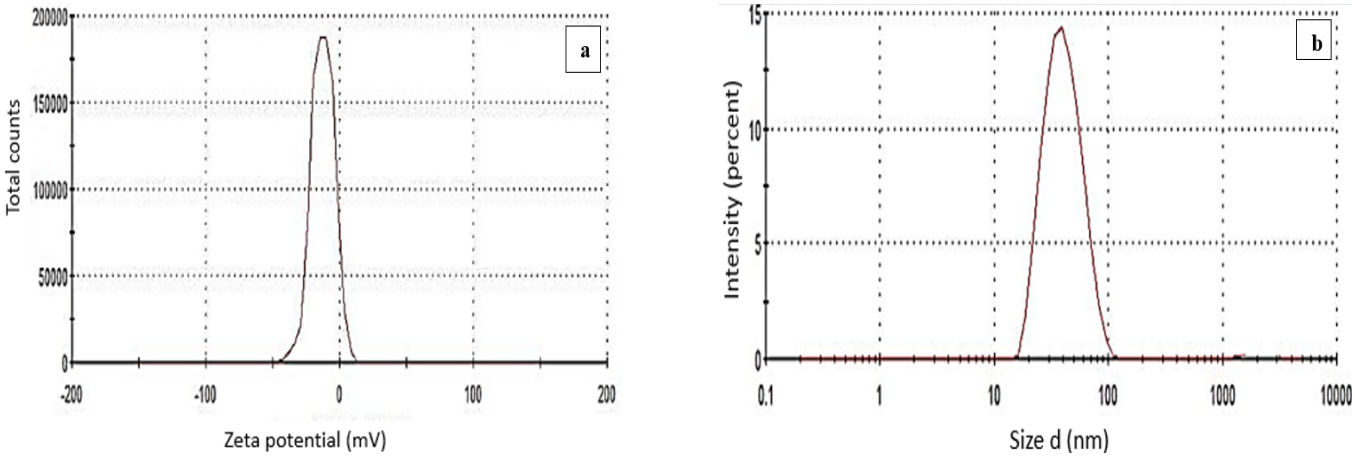

Figure 7. DLS analysis of NiO NPs (a) zeta potential, and(b) particle size

The maximum activity that appeared at 200 µg/ml was 16 mm ($p < 0.001$). The antibacterial assay's statistical findings are displayed in Figure 8. and Figure 9 presents a photographic plate inhibition zone.

The outcomes demonstrated that NiO NPs inhibited bacterial growth in concentration-dependent manner. These results are also presented in the previous study by Jassim *et al.* [56]. Nickel oxide nanoparticles (NiO NPs) are used in the biological field due to their cytotoxic effects and beneficial biological properties. The mechanism involves the release of Ni ions when NiO NPs come into contact with bacteria; these ions then adhere to the bacterial cell membrane. This process leads to an increase in reactive oxygen species (ROS) within the bacterial cell's lipid peroxides, weakening the cell membrane. This ultimately results in cell death due to changes in the bacterial strain's membrane permeability. NiO NPs can bind to bacteria and disrupt their permeability and respiration function, depending on the large surface area available for interaction. Bacterial growth and survival are influenced by the physio-chemical characteristics of NPs, which are largely resolute according to size, shape, and concentration [57]. The minimum inhibitory (MIC) is the concentration at which, after one day of culture, a bacterium will not grow visibly. When referring to conventional pharmaceutical antibiotics, mass concentration is used, such as µg/ml. MIC of NiO NPs was 25 µg/ml for both strains. These findings were most widely accepted and agreed with [58, 59]. The results obtained from this work were better than previous works in terms of using a small dose of the nanomaterial to obtain the same value from the inhibition zone as reported by Vijaya Kumar *et al.* [17].

6. CONCLUSION

In conclusion, NiO NPs were successfully manufactured using PLA, as confirmed by the characterization of their optical, chemical, zeta potential, and structural properties. XRD analysis was employed to identify the structure of FCC NiO NPs. Employing FTIR analysis, the existence of every functional group was determined. The FESEM study revealed that both NiO NPs had spherically shaped morphologies. The optical absorption spectra showed the NiO NPs have a wide band gap of 5.2 eV. The synthesized NiO NPs include both Ni and O, as validated by EDX analysis. NiO NPs showed moderate zeta potential values, and the particle size was 38.9 nm. NiO NPs show remarkable antibacterial efficacy against *S. aureus* and *E. coli,* which was approximately 16 mm for both. Investigation into the antibacterial properties of NiO NPs has helped in the development of NiO NPs as effective agents versus

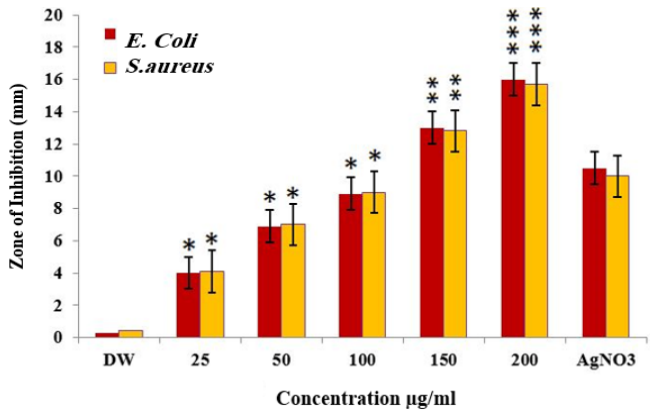

Figure 8. Antibacterial assay of NiO NPs vs. (*E. coli* and *S. aureus)*. Statistics are presented as (mean ± SD (*$p < 0.05$; **$p < 0.01$; ***$p < 0.001$); n = 3)

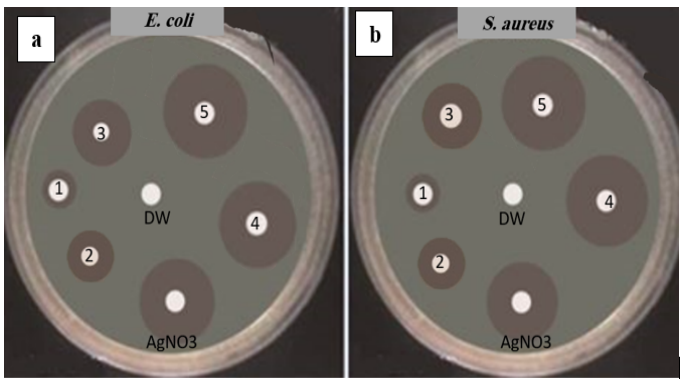

Figure 9. Zone of inhibition viewing the antibacterial test result of (a) *E. coli* (b) *S. aureus.* (1, 2, 3, 4, & 5 refer to the concentrations of NiO NPs (25, 50, 100, 150, and 200) µg/ml, respectively)

pathogenic bacteria in wounds, which highlights the promising role of NiO NPs in biomedical applications. Therefore, the obtained results emphasize the importance of NiO NPs made by a laser ablation technique in improving the overall effectiveness of antibacterial therapies and wound management strategies, and they suggest the necessity of further research and development in this field.

REFERENCES

[1] S. Ahmed, A. Hameed, and K. Al-Azawi, "Polymer-Impregnated Cement Mortar: Effects of PEG, PAM, and PVA on Mechanical Properties," *Journal of Applied Sciences and Nanotechnology*, vol. 4, no. 1, pp. 66–76, Feb. 2024, doi: 10.53293/jasn.2024.7089.1241.

[2] A. A. Yousif, N. F. Habubi, and A. A. Haidar, "Nanostructure Zinc Oxide with Cobalt Dopant by PLD for Gas Sensor Applications," *Journal of Nano- and Electronic Physics,* vol. 4, no. 2, pp. 020071–020076, 2012.

[3] A. J. Haider, A. D. Thamir, A. A. Najim, and G. A. Ali, "Improving Efficiency of TiO_2:Ag /Si Solar Cell Prepared by Pulsed Laser Deposition," *Plasmonics*, vol. 12, no. 1, pp. 105–115, Feb. 2017, doi: 10.1007/s11468-016-0235-0.

[4] A. Asha Radhakrishnan and B. Baskaran Beena, "Structural and Optical Absorption Analysis of CuO Nanoparticles," *Indian Journal of Advances in Chemical Science*, vol. 2, no. 2, pp. 158–161, 2014.

[5] J. A. S. Salman, A. A. Kadhim, and A. J. Haider, "Biosynthesis, Characterization and Antibacterial Effect of ZnO Nanoparticles Synthesized by Lactobacillus Spp," *Journal of Global Pharma Technology*, vol. 10, no. 3, pp. 348–355, 2018.

[6] B. Khameneh, R. Diab, K. Ghazvini, and B. S. Fazly Bazzaz, "Breakthroughs in bacterial resistance mechanisms and the potential ways to combat them," *Microbial Pathogenesis*, vol. 95, pp. 32–42, Jun. 2016, doi: 10.1016/j.micpath.2016.02.009.

[7] A. J. Haider, F. I. Sultan, M. J. Haider, and N. M. Hadi, "Spectroscopic and structural properties of zinc oxide nanosphere as random laser medium," *Applied Physics A*, vol. 125, no. 4, p. 260, Apr. 2019, doi: 10.1007/s00339-019-2529-5.

[8] Y. N. Slavin, J. Asnis, U. O. Häfeli, and H. Bach, "Metal nanoparticles: understanding the mechanisms behind antibacterial activity," *Journal of Nanobiotechnology*, vol. 15, no. 1, p. 65, Dec. 2017, doi: 10.1186/s12951-017-0308-z.

[9] R. Al-Obaidy, A. J. Haider, S. Al-Musawi, and N. Arsad, "Targeted delivery of paclitaxel drug using polymer-coated magnetic nanoparticles for fibrosarcoma therapy: in vitro and in vivo studies," *Scientific Reports*, vol. 13, no. 1, p. 3180, Feb. 2023, doi: 10.1038/s41598-023-30221-x.

[10] A. J. Haider, A. A. Jabbar, and G. A. Ali, "A review of Pure and Doped ZnO Nanostructure Production and its Optical Properties Using Pulsed Laser Deposition Technique," *Journal of Physics: Conference Series*, vol. 1795, no. 1, p. 012015, Mar. 2021, doi: 10.1088/1742-6596/1795/1/012015.

[11] S. F. Abbas, A. J. Haider, S. Al-Musawi, and M. K. Selman, "Antibacterial Effect of Copper Oxide Nanoparticles Prepared by Laser Production in Water Against Staphylococcus aureus and Escherichia coli," *Plasmonics*, vol. 19, no. 5, pp. 2401–2411, Oct. 2024, doi: 10.1007/s11468-023-02135-x.

[12] S. Abbas, A. Hadier, S. Al-Musawi, and B. Taha, "Synthesis of High-Performance Antibacterial Magnesium Oxide Nanostructures through Laser Ablation," *Journal of Applied Sciences and Nanotechnology*, vol. 4, no. 1, pp. 53–65, Feb. 2024, doi: 10.53293/jasn.2024.7213.1262.

[13] A. H. Attallah, F. S. Abdulwahid, Y. A. Ali, and A. J. Haider, "Enhanced Characteristics of Iron Oxide Nanoparticles for Efficient Pollutant Degradation via Pulsed Laser Ablation in Liquid," *Plasmonics*, vol. 19, no. 5, pp. 2581–2594, Oct. 2024, doi: 10.1007/s11468-024-02192-w.

[14] M. A. Behnajady and S. Bimeghdar, "Synthesis of mesoporous NiO nanoparticles and their application in the adsorption of Cr(VI)," *Chemical Engineering Journal*, vol. 239, pp. 105–113, Mar. 2014, doi: 10.1016/j.cej.2013.10.102.

[15] J. Huang, N. Zhu, T. Yang, T. Zhang, P. Wu, and Z. Dang, "Nickel oxide and carbon nanotube composite (NiO/CNT) as a novel cathode non-precious metal catalyst in microbial fuel cells," *Biosensors and Bioelectronics*, vol. 72, pp. 332–339, Oct. 2015, doi: 10.1016/j.bios.2015.05.035.

[16] R. Kumar, C. Baratto, G. Faglia, G. Sberveglieri, E. Bontempi, and L. Borgese, "Tailoring the textured surface of porous nanostructured NiO thin films for the detection of pollutant gases," *Thin Solid Films*, vol. 583, pp. 233–238, May 2015, doi: 10.1016/j.tsf.2015.04.004.

[17] P. Vijaya Kumar, A. Jafar Ahamed, and M. Karthikeyan, "Synthesis and characterization of NiO nanoparticles by chemical as well as green routes and their comparisons with respect to cytotoxic effect and toxicity studies in microbial and MCF-7 cancer cell models," *SN Applied Sciences*, vol. 1, no. 9, p. 1083, Sep. 2019, doi: 10.1007/s42452-019-1113-0.

[18] N. Talebian, M. Doudi, and M. Kheiri, "The anti-adherence and bactericidal activity of sol–gel derived nickel oxide nanostructure films: solvent effect," *Journal of Sol-Gel Science and Technology*, vol. 69, no. 1, pp. 172–182, Jan. 2014, doi: 10.1007/s10971-013-3201-8.

[19] M. Isa khan *et al.*, "Synthesis, characterization and antibacterial activity of NiO NPs against pathogen," *Inorganic Chemistry Communications*, vol. 122, p. 108300, Dec. 2020, doi: 10.1016/j.inoche.2020.108300.

[20] V. Helan *et al.*, "Neem leaves mediated preparation of NiO nanoparticles and its magnetization, coercivity and antibacterial analysis," *Results in Physics*, vol. 6, pp. 712–718, 2016, doi: 10.1016/j.rinp.2016.10.005.

[21] G. T. Anand, R. Nithiyavathi, R. Ramesh, S. John Sundaram, and K. Kaviyarasu, "Structural and optical properties of nickel oxide nanoparticles:

Investigation of antimicrobial applications," *Surfaces and Interfaces*, vol. 18, p. 100460, Mar. 2020, doi: 10.1016/j.surfin.2020.100460.

[22] S. T. Fardood, A. Ramazani, and S. Moradi, "A Novel Green Synthesis of Nickel Oxide Nanoparticles Using Arabic Gum," *Chemistry Journal of Moldova*, vol. 12, no. 1, pp. 115–118, May 2017, doi: 10.19261/cjm.2017.383.

[23] A. A. Ezhilarasi, J. J. Vijaya, K. Kaviyarasu, M. Maaza, A. Ayeshamariam, and L. J. Kennedy, "Green synthesis of NiO nanoparticles using Moringa oleifera extract and their biomedical applications: Cytotoxicity effect of nanoparticles against HT-29 cancer cells," *Journal of Photochemistry and Photobiology B: Biology*, vol. 164, pp. 352–360, Nov. 2016, doi: 10.1016/j.jphotobiol. 2016.10.003.

[24] M. Hafeez *et al.*, "Green Synthesis of Nickel Oxide Nanoparticles using Populus ciliata Leaves Extract and their Potential Antibacterial Applications," *South African Journal of Chemistry*, vol. 75, 2021, doi: 10.17159/0379-4350/2021/v75a21.

[25] A. B. Djurišić *et al.*, "Toxicity of Metal Oxide Nanoparticles: Mechanisms, Characterization, and Avoiding Experimental Artefacts," *Small*, vol. 11, no. 1, pp. 26–44, Jan. 2015, doi: 10.1002/smll. 201303947.

[26] S. F. Abbas, A. J. Haider, and S. Al-Musawi, "Antimicrobial and Wound Healing Effects of Metal Oxide Nanoparticles-Enriched Wound Dressing," *Nano*, vol. 18, no. 08, Jul. 2023, doi: 10.1142/S1793292023300050.

[27] Y. Khadim, U. Nayef, and F. Mutlak, "Enhancing Gas Sensing Performance through Laser Ablation Characterization of Silver@Gold Bimetallic Nanoparticles," *Journal of Applied Sciences and Nanotechnology*, vol. 4, no. 1, pp. 9–18, Feb. 2024, doi: 10.53293/jasn.2023.7137.1252.

[28] L. Armelao, D. Barreca, M. Bertapelle, G. Bottaro, C. Sada, and E. Tondello, "A sol–gel approach to nanophasic copper oxide thin films," *Thin Solid Films*, vol. 442, no. 1–2, pp. 48–52, Oct. 2003, doi: 10.1016/S0040-6090(03)00940-4.

[29] J. Zhang, J. Liu, Q. Peng, X. Wang, and Y. Li, "Nearly Monodisperse Cu_2O and CuO Nanospheres: Preparation and Applications for Sensitive Gas Sensors," *Chemistry of Materials*, vol. 18, no. 4, pp. 867–871, Feb. 2006, doi: 10.1021/cm052256f.

[30] S. Zaman, A. Zainelabdin, G. Amin, O. Nur, and M. Willander, "Efficient catalytic effect of CuO nanostructures on the degradation of organic dyes," *Journal of Physics and Chemistry of Solids*, vol. 73, no. 11, pp. 1320–1325, Nov. 2012, doi: 10.1016/j.jpcs. 2012.07.005.

[31] V. Amendola *et al.*, "Room-Temperature Laser Synthesis in Liquid of Oxide, Metal-Oxide Core-Shells, and Doped Oxide Nanoparticles," *Chemistry – A European Journal*, vol. 26, no. 42, pp. 9206–9242, Jul. 2020, doi: 10.1002/chem.202000686.

[32] N. A. Aljbar, B. R. Mahdi, A. H. Khalid, A. H. Attallah, F. S. Abdulwahid, and A. J. Haider, "Enhanced Surface Plasmon Resonance (SPR) Fiber Optic Sensor for Environmental Monitoring: A Coreless Fiber–Based Design," *Plasmonics*, vol. 20, no. 2, pp. 605–614, May 2024, doi: 10.1007/s11468-024-02332-2.

[33] A. J. Haider, A. D. Thamir, D. S. Ahmed, and M. R. Mohammad, "Deposition of silver nanoparticles on multiwalled carbon nanotubes by chemical reduction process and their antimicrobial effects," *AIP Conference Proceedings*, vol. 1758, no. 1, p. 030003, Jul. 2016, doi: 10.1063/1.4959399.

[34] T. Sasaki, Y. Shimizu, and N. Koshizaki, "Preparation of metal oxide-based nanomaterials using nanosecond pulsed laser ablation in liquids," *Journal of Photochemistry and Photobiology A: Chemistry*, vol. 182, no. 3, pp. 335–341, Sep. 2006, doi: 10.1016/j.jphotochem.2006.05.031.

[35] A. J. Haider, F. I. Sultan, and A. Al-Nafiey, "Controlled growth of different shapes for ZnO by hydrothermal technique," *AIP Conference Proceedings*, vol. 1968, no. 1, p. 030085, May 2018, doi: 10.1063/1.5039272.

[36] R. Al-Obaidy, A. Hadier, S. Al-Musawi, and N. Arsad, "Study of the Effects of Solution Types on Concentration of Iron Oxide by Pulsed Laser Ablation in Liquid," *Journal of Applied Sciences and Nanotechnology*, vol. 3, no. 1, pp. 137–150, Feb. 2023, doi: 10.53293/jasn.2022.5025.1172.

[37] A. H. Attallah, F. S. Abdulwahid, Y. A. Ali, and A. J. Haider, "Effect of Liquid and Laser Parameters on Fabrication of Nanoparticles via Pulsed Laser Ablation in Liquid with Their Applications: A Review," *Plasmonics*, vol. 18, no. 4, pp. 1307–1323, Aug. 2023, doi: 10.1007/s11468-023-01852-7.

[38] M. A. Al-Kinani, A. J. Haider, and S. Al-Musawi, "Design and Synthesis of Nanoencapsulation with a New Formulation of Fe@Au-CS-CU-FA NPs by Pulsed Laser Ablation in Liquid (PLAL) Method in Breast Cancer Therapy: In Vitro and In Vivo," *Plasmonics*, vol. 16, no. 4, pp. 1107–1117, Aug. 2021, doi: 10.1007/s11468-021-01371-3.

[39] H. Yamamoto, S. Tanaka, and K. Hirao, "Effects of substrate temperature on nanostructure and band structure of sputtered Co_3O_4 thin films," *Journal of Applied Physics*, vol. 93, no. 7, pp. 4158–4162, Apr. 2003, doi: 10.1063/1.1555681.

[40] A. J. Haider, T. Alawsi, M. J. Haider, B. A. Taha, and H. A. Marhoon, "A comprehensive review on pulsed laser deposition technique to effective nanostructure production: trends and challenges," *Optical and Quantum Electronics*, vol. 54, no. 8, p. 488, Aug. 2022, doi: 10.1007/s11082-022-03786-6.

[41] C. Diaz, M. L. Valenzuela, O. Cifuentes-Vaca, M. Segovia, and M. A. Laguna-Bercero, "Incorporation of NiO into SiO_2, TiO_2, Al_2O_3, and $Na_{4.2}Ca_{2.8}(Si_6O_{18})$ Matrices: Medium Effect on the Optical Properties and Catalytic Degradation of Methylene Blue," *Nanomaterials*, vol. 10, no. 12, p. 2470, Dec. 2020, doi: 10.3390/nano10122470.

[42] N. C. S. Selvam, R. T. Kumar, L. J. Kennedy, and J. J. Vijaya, "Comparative study of microwave and conventional methods for the preparation and optical properties of novel MgO-micro and nano-structures," *Journal of Alloys and Compounds*, vol. 509, no. 41, pp.

9809–9815, Oct. 2011, doi: 10.1016/j.jallcom.2011.08.032.

[43] K. Wongsaprom and S. Maensiri, "Synthesis and Room Temperature Magnetic Behavior of Nickel Oxide Nanocrystallites," *Chiang Mai Journal of Science*, vol. 40, no. 1, pp. 99–108, 2013.

[44] H. Qiao, Z. Wei, H. Yang, L. Zhu, and X. Yan, "Preparation and Characterization of NiO Nanoparticles by Anodic Arc Plasma Method," *Journal of Nanomaterials*, vol. 2009, no. 1, Jan. 2009, doi: 10.1155/2009/795928.

[45] N. A. Jawad and K. H. Hassan, "Structural Characterization of NiO Nanoparticles Prepared by Green Chemistry Synthesis Using Arundo donaxi Leaves Extract," *Journal of Physics: Conference Series*, vol. 1818, no. 1, p. 012007, Mar. 2021, doi: 10.1088/1742-6596/1818/1/012007.

[46] S. D. Khairnar and V. S. Shrivastava, "Facile synthesis of nickel oxide nanoparticles for the degradation of Methylene blue and Rhodamine B dye: a comparative study," *Journal of Taibah University for Science*, vol. 13, no. 1, pp. 1108–1118, Dec. 2019, doi: 10.1080/16583655.2019.1686248.

[47] Y.-G. Li, D.-H. Shi, H.-L. Zhu, H. Yan, and S. W. Ng, "Transition metal complexes (M=Cu, Ni and Mn) of Schiff-base ligands: Syntheses, crystal structures, and inhibitory bioactivities against urease and xanthine oxidase," *Inorganica Chim Acta*, vol. 360, no. 9, pp. 2881–2889, Jun. 2007, doi: 10.1016/j.ica.2007.02.019.

[48] G. Nabi *et al.*, "Structural, Optical, and Magnetic Properties of Pure and Vanadium-Doped NiO Microstructures for Spintronics Applications," *Journal of Superconductivity and Novel Magnetism*, vol. 34, no. 7, pp. 1801–1806, Jul. 2021, doi: 10.1007/s10948-020-05736-3.

[49] E. Hoseinzadeh *et al.*, "A Review on Nano-Antimicrobials: Metal Nanoparticles, Methods and Mechanisms," *Current Drug Metabolism*, vol. 18, no. 2, pp. 120–128, Mar. 2017, doi: 10.2174/1389200217666161201111146.

[50] G. Basak, D. Das, and N. Das, "Dual Role of Acidic Diacetate Sophorolipid as Biostabilizer for ZnO Nanoparticle Synthesis and Biofunctionalizing Agent Against Salmonella enterica and Candida albicans," *Journal of Microbiology and Biotechnology*, vol. 24, no. 1, pp. 87–96, Jan. 2014, doi: 10.4014/jmb.1307.07081.

[51] M. Rubinstein, R. H. Kodama, and S. A. Makhlouf, "Electron spin resonance study of NiO antiferromagnetic nanoparticles," *Journal of Magnetism and Magnetic Materials*, vol. 234, no. 2, pp. 289–293, Sep. 2001, doi: 10.1016/S0304-8853(01)00313-4.

[52] S. Rakshit, S. Ghosh, S. Chall, S. S. Mati, S. P. Moulik, and S. C. Bhattacharya, "Controlled synthesis of spin glass nickel oxide nanoparticles and evaluation of their potential antimicrobial activity: A cost effective and eco friendly approach," *RSC Advances*, vol. 3, no. 42, p. 19348, 2013, doi: 10.1039/c3ra42628a.

[53] A. Fouda *et al.*, "The Antimicrobial and Mosquitocidal Activity of Green Magnesium Oxide Nanoparticles Synthesized by an Aqueous Peel Extract of Punica granatum," *Chemistry (Easton)*, vol. 5, no. 3, pp. 2009–2024, Sep. 2023, doi: 10.3390/chemistry5030136.

[54] S. F. Abbas, A. J. Haider, S. Al-Musawi, and M. K. Selman, "Impact of laser parameters on synthesis zinc oxide nanoparticles and evaluation of its antibacterial activity," *Optical and Quantum Electronics*, vol. 56, no. 5, p. 901, Apr. 2024, doi: 10.1007/s11082-024-06719-7.

[55] M. Danaei *et al.*, "Impact of Particle Size and Polydispersity Index on the Clinical Applications of Lipidic Nanocarrier Systems," *Pharmaceutics*, vol. 10, no. 2, p. 57, May 2018, doi: 10.3390/pharmaceutics10020057.

[56] S. M. Jassim, M. A. Abd, and I. A. Hammed, "Green synthesis of Nickel Oxide Nanoparticles using Syzygium Aromatic Extract: Characterization and Biological Applications," *Al-Bahir*, vol. 2, no. 2, Apr. 2023, doi: 10.55810/2313-0083.1024.

[57] V. Gupta, V. Kant, A. Gupta, and M. Sharma, "Synthesis, characterization and concentration dependant antibacterial potentials of nickel oxide nanoparticles against Staphylococcus aureus and Escherichia coli," *Nanosystems: Physics, Chemistry, Mathematics*, vol. 11, no. 2, pp. 237–245, Apr. 2020, doi: 10.17586/2220-8054-2020-11-2-237-245.

[58] S. Srihasam, K. Thyagarajan, M. Korivi, V. R. Lebaka, and S. P. R. Mallem, "Phytogenic Generation of NiO Nanoparticles Using Stevia Leaf Extract and Evaluation of Their In-Vitro Antioxidant and Antimicrobial Properties," *Biomolecules*, vol. 10, no. 1, p. 89, Jan. 2020, doi: 10.3390/biom10010089.

[59] N. Behera *et al.*, "Oxidative stress generated at nickel oxide nanoparticle interface results in bacterial membrane damage leading to cell death," *RSC Advances*, vol. 9, no. 43, pp. 24888–24894, 2019, doi: 10.1039/C9RA02082A.